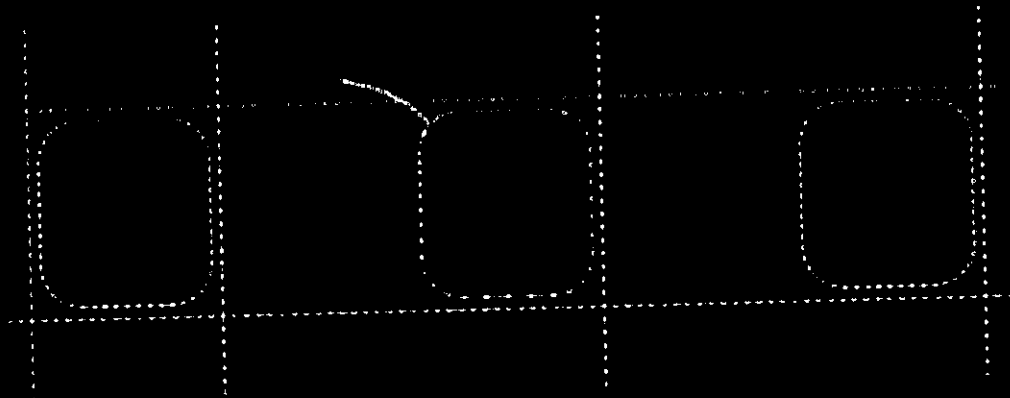


Topics in Engineering Vol. 33

Boundary Element Methods for Damage Tolerance Design of Aircraft Structures

N. Salgado



**Computational Mechanics Publications
Southampton UK and Boston USA**

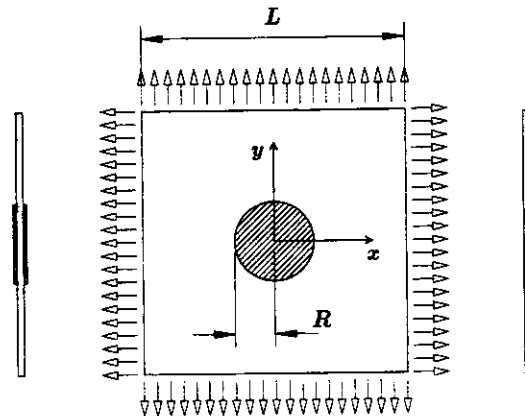


Figure 7-6: A large square sheet bonded with a single circular patch (on the right) or double circular patches (on the left).

to the use of the DBEM, re-meshing after each crack increment is reduced to adding new elements to the crack boundary. No changes are required to the existing mesh. Moreover, only matrix coefficients due to the new elements have to be calculated and added, as new rows and columns, to the existing (LU-decomposed) matrix. Only the new rows and columns have to be decomposed during the current increment and the computational time is substantially reduced.

The crack propagation analysis for adhesively patched sheets retains all the features and advantages listed in the previous paragraph, because the crack boundaries can be excluded from the attachment region boundary (as demonstrated in Section 7.4) and therefore *no change is required* to the existing *attachment mesh* after each analysis increment.

7.6 Numerical Examples

7.6.1 Single or Double Circular Patch Bonded to a Square Sheet

A square sheet of side $L = 200$ mm is subjected to biaxial stresses as shown in Figure 7-6 ($\sigma = 1$ GPa). The sheet has thickness 1.5 mm. The sheet material has Young's modulus $E = 70$ GPa and Poisson's ratio $\nu = 0.3$. A single circular patch of radius $R = 30$ mm, 1.5 mm thick, of the same material as the sheet and with an unloaded boundary, is bonded to the centre of the sheet by means of an adhesive layer of thickness $h_A = 0.15$ mm and shear modulus $G_A = 0.6$ GPa (detail on the right hand side of Figure 7-6). The adhesive layer locus encloses the whole patch domain (i.e. the attachment region boundary coincides with the patch boundary). The single patch problem was analysed using different discretizations, each corresponding to a different number of internal points (45, 69, 109 and 145), regularly distributed throughout the attachment region. Figure 7-7 shows the discretization containing 145 internal points. Displacement boundary conditions were applied to the sheet in order to constrain rigid body movements. Patch rigid body movements were naturally constrained by the imposition of displacement compatibility with the sheet.

Results for the attachment shear forces (τ) are presented in Figure 7-8 normalized with

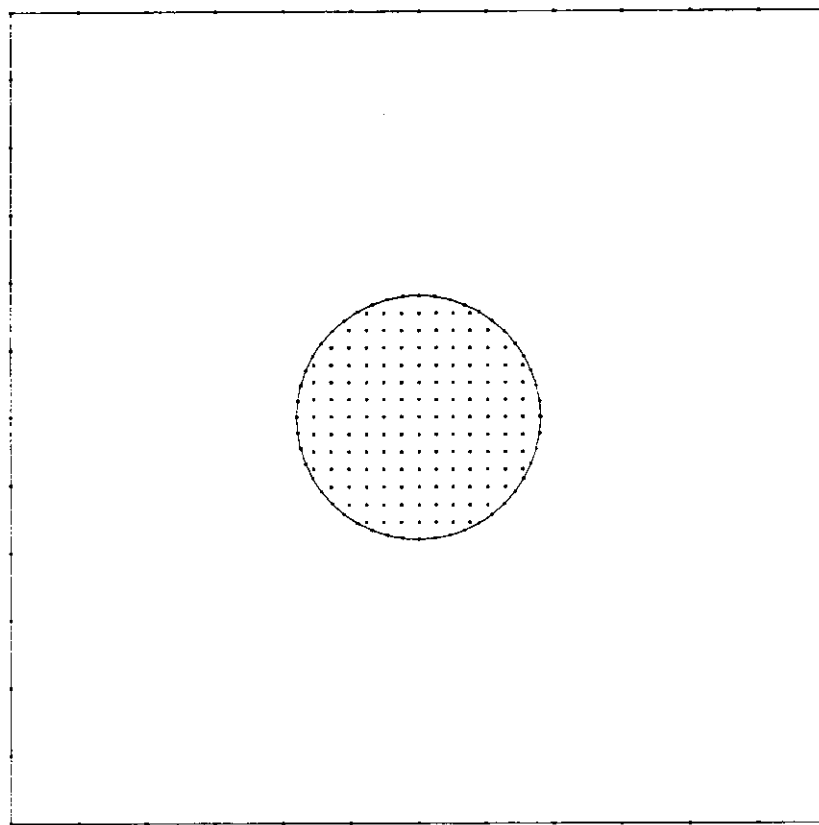


Figure 7-7: Mesh containing 145 internal points for analysis of circular patch bonded to large square sheet.

respect to the sheet far field stresses ($\sigma_x = \sigma_y = 1$ GPa). On the right hand side of Figure 7-8, results obtained for different discretizations are compared with the analytic solution for an infinite sheet subjected to hydrostatic traction [126]. It can be seen that good agreement was obtained even for relatively coarse internal points grids. Refining the boundary mesh was found not to affect the results significantly (i.e. doubling the number of elements resulted in the maximum shear stress changing by less than 1%).

If, instead of one patch 1.5 mm thick, two patches 0.75 mm thick are bonded either side of the sheet (see detail on the left of Figure 7-6), the attachment forces reduce slightly, as shown on the left hand side of Figure 7-8. For the analysis of this case, two patches with identical external boundaries were modelled. The boundary and internal point discretization is identical to that presented in Figure 7-7.

7.6.2 Single or Double Circular Patch Bonded to a Cracked Sheet

A square sheet of side $L = 200$ mm is subjected to uniform tensile stress in the y -direction as shown in Figure 7-9 ($\sigma = 1$ GPa). The sheet contains a central crack at $y = 0$, -15 mm $\leq x \leq 15$ mm ($a = 15$ mm). The sheet thickness is 1.5 mm and its material has Young's

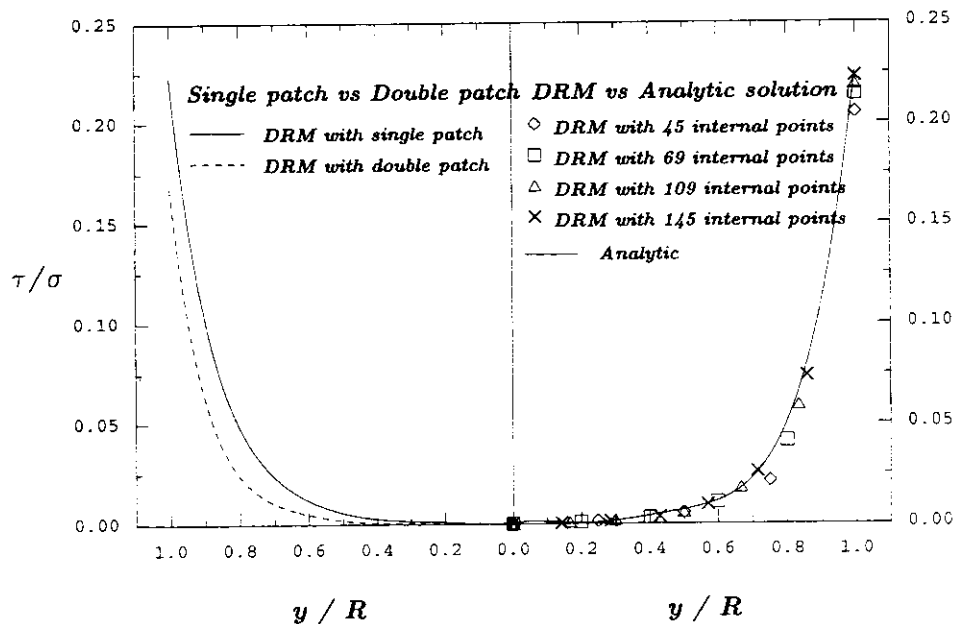


Figure 7-8: Normalized attachment shear stresses for a circular patch bonded to a large square sheet. On the right, results are compared to analytical solution for infinite sheet. On the left, comparison is made between attachment shear stresses resulting from the use of a double patch instead of a single patch.

modulus $E = 70$ GPa and Poisson's ratio $\nu = 0.3$. The sheet is patched with either a single patch, 1.5 mm thick (see top of Figure 7-9), or double patches, 0.75 mm thick (see bottom of Figure 7-9), so that the relative stiffness between the sheet and reinforcement is the same in both cases. The patches are circular and have radius $R = 30$ mm. They are made of the same material as the sheet. An adhesive layer of thickness $h_A = 0.15$ mm and shear modulus $G_A = 0.6$ GPa is used to attach the patches to the sheet.

The adhesive layer locus encloses the whole patch domain. However, the attachment region boundary does not include the crack boundary (see Section 7.4) and is taken to be the same as the patch boundary. Displacement boundary conditions were applied to the sheet in order to constrain rigid body movements. Patch rigid body movements were naturally constrained by the imposition of displacement compatibility with the sheet.

The single patch problem was analysed using different discretizations, each corresponding to a different number of internal points, regularly distributed throughout the attachment region. The sheet and patch boundary meshes were found to have a much less significant influence on the convergence of the results than the patch internal point discretization.

The attachment shear stresses (τ) over the y axis ($x = 0$) are presented on the right hand side of Figure 7-10, normalized with respect to the sheet far field stresses ($\sigma = 1$ GPa). As expected, the shear stresses are higher near the crack ($y/R = 0$) and patch boundary ($y/R = 1$). It can be seen that good agreement was obtained between the solutions calculated for different discretizations. On the left hand side of Figure 7-10 a comparison is made with

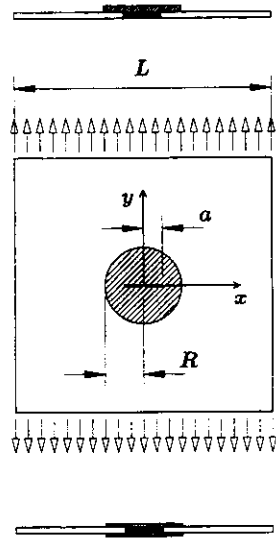


Figure 7-9: Large cracked square sheet reinforced with a single circular patch (on top) or double circular patches (on bottom).

the shear stresses obtained for the double patch solution. In that case, 294 internal points were used and the shear stresses are slightly lower than those for the single patch.

It was observed that convergence is slow for the stress intensity factor when regular internal point grids are refined. However, much faster convergence can be obtained if an irregular distribution of internal points, finer in the vicinity of the crack tip, is refined. An example of such discretization containing a total of 218 internal points is presented in Figure 7-11. The Figure also illustrates the sheet and patch boundary meshes used throughout the example. A converged stress intensity factor for the single patch solution was obtained with 426 internal points as $K_I^{\text{single}}/K_0 = 0.213$ ($K_0 = \sigma\sqrt{\pi a}$). The value is within 2% of the one presented by Young *et al.* [125], which was calculated using 116 square constant internal cells.

The double patch solution was analysed with the discretization (boundary and internal) presented in Figure 7-11 and compared to the value obtained for the single patch with the same mesh. The stress intensity factor obtained is such that $K_I^{\text{double}}/K_I^{\text{single}} = 0.63$. Although the result for the single patch is about 3% higher than the converged solution obtained with 426 internal points, the relation $K_I^{\text{double}}/K_I^{\text{single}}$ can be regarded as reliable, as both values were calculated using the same mesh.

7.6.3 Cases Involving a Circular Patch, a Square Sheet, Cracks and Holes

A square sheet and a single circular patch are bonded to each other. The dimensions, external load, material properties and the adhesive layer properties are identical to those in the previous example. A series of configurations involving the presence of a circular hole, either in the sheet or in the patch or in both, and a central crack in the sheet are considered. They include:

1. a sheet without a hole and without a crack and a patch without a hole;
2. a sheet without a hole and without a crack and a patch with a hole;

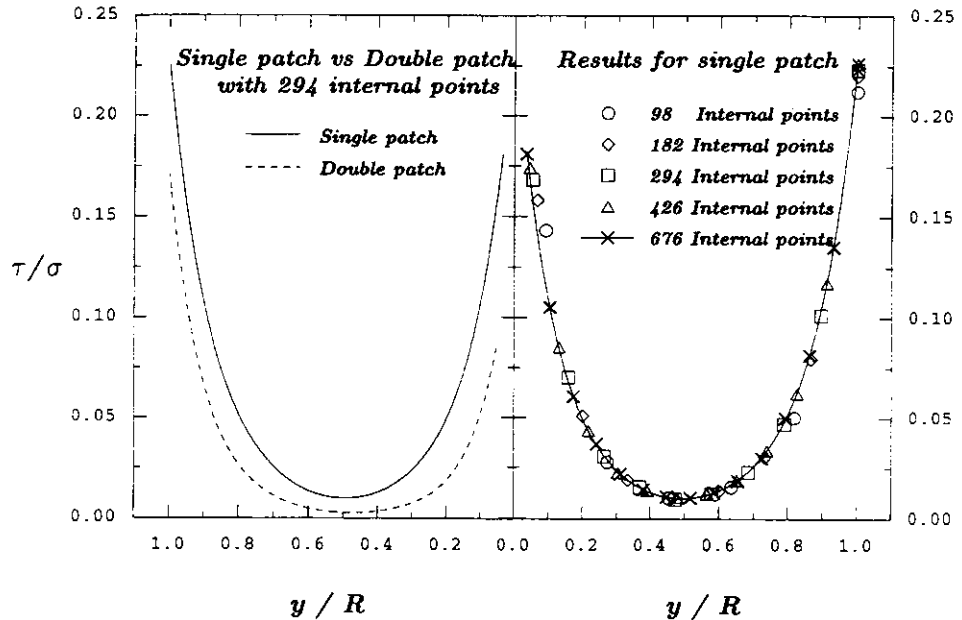


Figure 7-10: Normalized attachment shear stresses for a large patched square sheet containing a central crack. On the right, results are obtained with different discretization, involving a different number of internal points. On the left, comparison is made between attachment shear stresses resulting from the use of double patches instead of a single patch.

3. a sheet with a hole and a patch without a hole;
4. a sheet with a hole and a patch with a hole;
5. a sheet with a crack and a patch without a hole;
6. a sheet with a crack and a patch with a hole;
7. a sheet with a cracked hole and a patch without a hole;
8. a sheet with a cracked hole and a patch with a hole.

Figure 7-12 illustrates the case when the sheet contains a central cracked hole and the patch contains a central circular hole (case 8). The hole has radius $R_h = 10$ mm and the total crack length measured from the centre of the hole is $a = 15$ mm. In the cases when only the crack is present in the sheet (cases 6 and 7), it is a central one with $a = 15$ mm, exactly as in the previous example.

The attachment region boundary coincides with the crack boundary, except for the cases where the sheet contains the hole and the patch does not. The crack is never included in the attachment region boundary. The discretization used in all cases is similar to that presented in Figure 7-13, which involves 252 internal points.

The attachment shear stresses, over the y axis ($x = 0$), are presented in Figure 7-14, normalized with respect to $\sigma = 1$ GPa. For case 1, the shear stresses tend to zero at the centre of the configuration ($y/R = 0$) and to a maximum value at the edge of the patch ($y/R = 1$). The addition of a crack to the sheet (case 5) causes the shear stresses to increase in the direction of the crack boundary at the centre of the configuration ($y/R = 0$). If the